Frequency Band Gaps in Dielectric Granular Metamaterials Modulated By Electric Field

Nima Nejadsadeghi[1], Luca Placidi[2,3], Maurizio Romeo[4] and Anil Misra[5]*

[1]Mechanical Engineering Department,
University of Kansas, 1530 W. 15th Street, Learned Hall, Lawrence, KS 66045-7609.
[2]International Telematic University Uninettuno, Rome, Italy;
[3]International Research Center on Mathematics and Mechanics of Complex System, Università degli Studi dell' Aquila, Italy
[4]DIMA, Università degli Studi di Genova, Genoa, Italy
[5]Civil, Environmental and Architectural Engineering Department,
University of Kansas, 1530 W. 15th Street, Learned Hall, Lawrence, KS 66045-7609.
*corresponding author: Ph: (785) 864-1750, Fax: (785) 864-5631, Email: amisra@ku.edu

in:

Mechanics Research Communications

Abstract

Wave propagation in granular materials is known to be dispersive. Micromorphic continuum model based upon granular micromechanics [1] has the ability to describe this dispersion behavior. In this paper we show that the dispersive behavior can be modulated by using electric field when the grains have dielectric properties. To this end, we apply the recently enhanced model that incorporates electro-elastic coupling by connecting microstrain to electric dipole and quadrupole densities due to bound charges in dielectric grains [2]. We particularly investigate the effect of induced polarization that arises due to an imposed electric field. Two cases of dielectric one dimensional infinite rods with the same micromorphic properties have been studied, where case 1 and 2 are in null and nonzero external electric fields, respectively. Parametric studies are performed to understand the contribution of the polarizability (dipole effect), intrinsic quadrupole density, and external electric field on the dispersive behavior of granular media. Results predict an acoustic and an optical branch in the dispersive curve. Polarizability and external electric field are mainly affecting small wavenumber behavior of the wave branches, while quadrupole density alters the behavior of the material at large wavenumbers. A possibility of altering the optical branch to an acoustic branch is also observed, for which instability or attenuation occurs depending upon the direction of the imposed electric field with respect to the wave propagation direction. We find that the location and the width of the frequency band gaps can be altered using external electric field. The possibility of creating or removing frequency band gaps is also shown to exist. The extended theory accounting for electro-elasticity can therefore be utilized as a tool to analyze existing granular media, or to design granular metamaterials, as it systematizes the design process and eliminates ad-hoc manners leading to large data libraries.

Keywords: Granular micromechanics; Micromorphic continua; electro-elasticity; tunable metamaterial; frequency band gaps; wave dispersion.

1. Introduction

Granular solids are ubiquitous and impact diverse areas of engineering and science such as material development, transportation and infrastructure systems [3, 4], pharmaceuticals and drug delivery, and natural processes in geophysics, with applications including, but not limited to wave attenuation and energy harvesting devices, as recent studies on granular crystals have shown [5-8]. The granular micromechanics based micromorphic continuum model introduced in [1] has the ability to describe and predict natural or synthetic granular materials (metamaterials) behavior and can be used as a tool to design and analyze granular materials. The proposed continuum model also provides the freedom to describe the average behavior of many micro-structures that are being currently proposed by combining masses, linear springs, rotational springs, beams etc. (see for example [9-11]). Extending this model to account for electro-elasticity coupling seems essential because of the numerous potential engineering applications which include sensors, actuators, acoustic metamaterials, and ultra-sound imagers [12-14]. This extended theory is not only beneficial to give a comprehensive description of the involved physics resulting in a particular effect, but also crucial as a tool for developing new materials with desired behavior. To describe electro-elasticity effects in granular materials and granular metamaterials it is necessary to take into account the coupling of the mechanical deformation and electric charge displacements in the material's internal (micro-) structure [2, 15, 16]. A micromorphic theory of electro-magnetic non-conducting (dielectric) materials has recently been published [2], having cast a consistent continuum description of polarization and magnetization. In this paper, the granular micromechanics based micromorphic continuum model [1] equipped with the electro-elasticity coupling effect developed for non-conducting materials introduced in [2] is used to study the dispersive behavior of the granular materials in response to the elastic deformation waves subjected to a constant electric field in a quasi-electro-static case. Using this theory, the classical linear hyperbolic partial differential wave equation becomes intricate because of the additional terms introduced to account for the micro-mechano-morphology and electro-elasticity coupling. An understanding of the effects of the electro-elasticity coupling on the behavior of granular materials proves indispensable for both describing the behavior of existing natural granular materials, and designing metamaterials with desired objectives.

The paper is organized as follows. An overview of the theory is presented in section 2, where the kinematics of the model and the variational approach to derive the governing equations of motion are introduced. To avoid complexities, and to be better able to interpret the effects of the electro-elasticity in the dispersive behavior of the granular materials, we limit our studies to two cases of longitudinal wave propagation in one dimensional infinite rods. Section 3 describes the analysis for two cases with equal microstructural properties. Cases 1 and 2 are in null and nonzero external electric fields, respectively. We perform extensive studies to emphasize the effect of micro- and macro-scale parameters on the dispersive behavior of the material. Section 4 is devoted to the summary of the work done in this paper, along with a discussion on the potential applicability of the theory used here in the design and fabrication of metamaterials with specific material properties for particular purposes.

2. Micromorphic Model based upon Granular Micromechanics

The granular micromechanics proceeds from an identification of the grain-scale motions in terms of the continuum measures and the volume average of grain-pair interaction energies with the macro-scale deformation energy density, in an approach reminiscent of developments in continuum modeling presented by Piola [17]. In the current format of granular micromechanics [18], two grain-scale kinematic measures are defined, one for determining relative displacements and the other for relative rotations. It is remarkable that the considered grain-scale kinematic measures represent the combined effect of the grain centroid displacement, spin and size, and do not follow the decomposition adopted in some previous attempts of micro-macro identifications [19, 20]. These grain-scale motions are identified with six set of continuum kinematic measures that include the macro-scale displacement/rotation gradients, micro-scale displacement/rotations gradients identified with displacement/rotation fluctuations within a material point, and macro-gradient of the micro-scale displacement/rotation gradients. The deformation energy density of a material point is then expressed in terms of the kinematic measures at the two scales and the inter-granular force measures as well as the continuum stress are defined as conjugates of the kinematic measures. Subsequently, the relationships are derived between stress and inter-granular forces that include stretch/compression, tangential, bending and torsional actions as well as for further derivation of the constitutive relations, variational principle, and balance equations for non-

classical micromorphic model whose parameters can be identified in terms of the grain-scale properties [1, 21, 22].

To develop a continuum description, each material point is considered a volume element (VE), as shown in Figure 1. Let the coordinate system, x, be considered in the global (macro-scale) model, and attach a local or micro-scale coordinate system, x', to the material point P or the barycenter of the VE with its axes parallel to the global coordinate system axes. The micro-scale coordinate system is defined such that it is able to distinguish different grains inside the material point. The displacement of the grains are then not only a function of the coordinates of the material point P, but also of the micro-scale coordinates of the grain within the material point, i.e.,

$$\phi_i = \phi_i(x, x') \tag{1}$$

where ϕ_i is the displacement of grain centroids. Now consider the displacement, ϕ_i^p, of the centroid of grain, p, contained within the continuum material point, where the displacement is defined in [1]. Utilizing the Taylor's expansion, this displacement can be related to the displacement, ϕ_i^n, of the centroid of neighboring grain, n, such that the difference will be the relative displacement, δ_i^{np}, of the two grains, which is given as follows, where we have included the first and second order terms in the Taylor series expansion,

$$\delta_i^{np} = \phi_i^p - \phi_i^n = \phi_{i,j}^n l_j + \frac{1}{2}\phi_{i,jk}^n l_j l_k + \cdots \tag{2}$$

where l_j is the vector joining the centroids of n and p. Following a similar analysis, the relative rotations of two interacting grains, n and p, denoted by θ_i is found as [1]

$$\theta_i^{np} = e_{jki}\phi_{k,jp} l_p \tag{3}$$

where e_{ijk} is permutation symbol. Note that the summation convention over repeated indices (in the subscript) is implied unless noted otherwise.

By introducing the decomposition of the displacement gradient field into an average field, $\bar{\phi}_{i,j}$, and a fluctuation field, γ_{ij}, as [1, 23]

$$\psi_{ij} = \phi_{i,j} = \bar{\phi}_{i,j} - \gamma_{ij} \tag{4}$$

the relative displacement of grains p and n can be decomposed as

$$\delta_i^{np} = \bar{\phi}_{i,j} l_j - \gamma_{ij} l_j + \frac{1}{2}\phi_{i,jk} l_j l_k + \cdots \qquad \delta_i^m + \delta_i^g \tag{5}$$

Conjugate to each gradient term in Eq. 2 and 4, stress measures may be defined. Similarly force/moment measures conjugate to each grain-scale relative displacement/rotation term in Eq. 2 and 4 may be introduced (see [1]). Furthermore, for linear elasticity, the micro-scale deformation energy is formulated as quadratic functions of the grain-pair kinematic measures introduced in Eq. 2 and 4, which requires introduction of four different inter-granular stiffness measures defined as $K_q^p; G_q^u$ where K and G denote the stretch and rotational stiffnesses, respectively, *p=M, m* and *g*; *q=n, w*; *M* denotes macro-stiffness; *m* denotes the micro-stiffness; *g* denotes the second gradient stiffness; *u* denotes the rotation; and the subscripts *n* and *w* refer to the normal and tangential grain-pair interaction directions. The macro-scale constitutive moduli tensors, $\mathbf{C}^{\mathrm{M}}$, $\mathbf{C}^{\mathrm{m}}$, $\mathbf{A}^{\mathrm{g}}$, and $\mathbf{A}^{\mathrm{u}}$ are then obtained in terms of these inter-granular stiffness measures.

To account for the electro-elasticity coupling effect, bound charge micro-density $\sigma'(x,x')$ representing the bound charges in dielectric grains, is introduced. The charge density σ, which is a volume average of the charge micro-density, is zero for dielectric materials, but this does not prevent the existence of nonzero electric dipole density *p* and quadrupole density *Q*, defined as functions of micro-deformation [2]. Polarization as a function of dipole and quadrupole densities is introduced, and subsequently, electric displacement can be defined in the usual manner [2]. The energy density coming from the electric field can be accounted for using a micro-density Lorentz force. To this end, the mean dipole density of a VE of granular media is estimated in the form $p_i = \alpha E_i^{(0)}$ [24] where $E_i^{(0)}$ is the constant electric field vector and α is the equivalent polarizability constant related to the number of grains in the VE and the grains intrinsic dipole, while the quadrupole density is estimated in terms of quadrupole intrinsic to the dielectric grains in an analogy to the microinertia [2]. Thus formulated electric energy density with added terms to account for the electro-elasticity coupling in terms of polarization is then used, and

subsequently, the principle of stationary action can be applied to find the governing equations of motions. For an electrostatic case, the governing equations then take the form:

$$\left(C^{M}_{ijkl}+C^{m}_{ijkl}\right)\bar{\phi}_{k,lj}-C^{m}_{ijkl}\psi_{kl,j}-\alpha E^{(0)}_{k}\varphi_{,ik}-\frac{1}{2}\bar{Q}_{jk}\varphi_{,ikj}=\rho\ddot{u}_{i} \tag{6a}$$

$$\begin{aligned}&\left(A^{g}_{jkilmn}+A^{u}_{jkilmn}\right)\psi_{lm,ni}+C^{m}_{jklm}\bar{\phi}_{l,m}-C^{m}_{jklm}\psi_{lm}\\&+\alpha E^{(0)}_{j}\left(E^{(0)}_{k}-\varphi_{,k}\right)+\alpha E^{(0)}_{l}E^{(0)}_{k}\psi_{jl}-\bar{Q}_{jl}\varphi_{,kl}=I\ddot{\psi}_{ij}\end{aligned} \tag{6b}$$

$$-\varphi_{,ii}+\alpha E^{(0)}_{l}\psi_{il,i}-\bar{Q}_{lm}\psi_{il,im}=0 \tag{6c}$$

where the noncontact mechanical volumic forces and double forces are assumed to be absent, ρ and I are the overall density and micro-inertia [1], respectively, of the granular medium, $\bar{Q}$ is the mean quadrupole density in the representative volume element, and φ is the scalar electric potential [2]. This term arises from separation of the electric field in the present quasi-electrostatic case as $E=E^{(0)}-\nabla\varphi$ where $E^{(0)}$ is the fixed applied field and the scalar potential φ is responsible for the dynamic contribution. The micro-inertia depends on the representative volume element (RVE). The micro-volume can consist of one or more grains, depending on the assumed RVE. In practice, an RVE is a collection of grains that can be stacked to develop the whole structure. Therefore, the RVE size depends on the granular fabric tensor, and intergranular interaction mechanism. If the granular structure is homogenous in both fabric tensor (geometrical aspect) and grain-pair interactions, the RVE can be assumed to have only one grain (for example a 2D hexagonal structure with no defects and with equal grain-pair interaction in every direction, such as [25]). However, taking an RVE with only one grain results in loss of degrees of freedom introduced in the micromorphic theory, and the theory simplifies to the classical continuum mechanics theory. The governing equations Eqs. 6 have been derived using an energy approach where the virtual work of electrical body forces derived from the Lorentz force in the micromorphic description of polarization have been included in a micromorphic continua obtained from granular micromechanics based homogenization framework. Eq. 6a and 6b are displacement equations of motion derived in [1] with terms accounting for the electro-elasticity coupling, and Eq. 6c represents the Gauss's law. The Ampere's law in the quasi-static case decouples from the governing equations Eq. 6.

3. Longitudinal wave propagation in a one dimensional granular rod

3.1. Mathematical Formulation

In what follows, we consider the longitudinal (P) wave propagation along x_1 axis in an isotropic one dimensional infinite rod formed of dielectric grains. In this case, the solutions of Eq. 6 are of the form

$$\bar{\phi}_1 = \bar{\phi}_1(x_1,t), \quad \psi_{11} = \psi_{11}(x_1,t), \quad \varphi_{11} = \varphi_{11}(x_1,t) \tag{7}$$

and the governing equations in Eq. 6 reduce to

$$(P+Q)\bar{\phi}_{1,11} - Q\psi_{11,1} - \alpha E_1^{(0)}\varphi_{,11} - \frac{1}{2}\bar{Q}_{11}\varphi_{,111} = \rho\ddot{\ } \tag{8a}$$

$$R\psi_{11,11} + Q\bar{\phi}_{1,1} - Q\psi_{11} + \alpha E_1^{(0)}E_1^{(0)} - \alpha E_1^{(0)}\varphi_{,1} + \alpha E_1^{(0)}E_1^{(0)}\psi_{11} - \bar{Q}_{11}\varphi_{,11} = I\ddot{\ } \tag{8b}$$

$$-\varphi_{,11} + \alpha E_1^{(0)}\psi_{11,1} - \bar{Q}_{11}\psi_{11,11} = 0 \tag{8c}$$

where the symbols of P, Q, and R, following [26], have been used for brevity, and have the values of C^M_{1111}, C^m_{1111}, and A^g_{111111}, respectively, and $\bar{Q}_{11}$ is the mean quadrupole density in the representative volume element.

The solution for the system of partial differential equations in Eq. 8 consists of two parts – the general and the particular, satisfying the homogenous and the non-homogenous forms of Eq. 8, respectively. The homogenous solution is formed of the plane wave functions. The particular solution depends upon the term, $\alpha E_1^{(0)}E_1^{(0)}$, a body force induced by the electric field independent of $\bar{\phi}_1$ and ψ_{11}, and does not contribute to the eigen solutions. Therefore, we focus only upon the general solution of Eq. 8. Specializing the solutions in Eq. 8 to plane waves [23], and only considering progressing waves, and accounting for the coupling between electric potential and mechanical deformation for a coherent plane-wave problem, we will have the following oscillatory form for the solutions of Eq. 8

$$\bar{\phi}_1 = \mathrm{Re}\left(A_1 i\, \mathrm{e}^{i(kx_1-\omega t)} \right), \quad \psi_{11} = \mathrm{Re}\left(B_{11}\, \mathrm{e}^{i(kx_1-\omega t)} \right), \quad \varphi = \mathrm{Re}\left(C\, \mathrm{e}^{i(kx_1-\omega t)} \right) \tag{9}$$

where k is the wavenumber, ω is the frequency, iA_1 and B_{11} are the amplitudes of the macro-displacement and micro-displacement gradient, respectively, and C is the amplitude of the potential function. Substituting for φ from Eq. 9 in Eq. 8c gives

$$C = \left(-\bar{Q} - i\frac{\alpha E_1^{(0)}}{k} \right) B_{11} \tag{10}$$

Using Eq. 9 and 10, we can rewrite Eq. 8a and 8b in the following matrix form

$$\begin{bmatrix} c_0^2 k^2 & \frac{d^2}{2}k^3 - i\frac{\alpha c_3 d}{2}k^2 + \left(c_A^2 + \alpha^2 c_3^2\right)k \\ \frac{k}{p^2} & \left(c_1^2 + c_2^2\right)k^2 + \frac{1}{p^2} + \frac{\alpha^2 c_3^2}{c_A^2 p^2} - \frac{\alpha c_3^2}{c_A^2 p^2} \end{bmatrix} \begin{bmatrix} A_1 \\ B_{11} \end{bmatrix} = \omega^2 \begin{bmatrix} A_1 \\ B_{11} \end{bmatrix} \tag{11}$$

where, following [26], we have introduced the velocities c_0, c_1, and c_A, characteristic time, p, written as

$$c_0^2 = \frac{P+Q}{\rho}, \quad c_1^2 = \frac{R}{I}, \quad c_A^2 = \frac{Q}{\rho}, \quad p^2 = \frac{I}{Q} \tag{12}$$

as well as a new velocities c_2 and c_3 and the parameter d as

$$c_2^2 = \frac{\bar{Q}^2}{I}, \quad c_3 = \frac{E_1^{(0)}}{\sqrt{\rho}}, \quad d^2 = \frac{\bar{Q}^2}{\rho} = p^2 c_2^2 c_A^2 \tag{13}$$

We remark that c_3 has the dimension of velocity due to the use of Heaviside-Lorentz units, and has been introduced so as to inherit the sign of the applied electric field. Further, it is noteworthy that parameter d is not independent, and interestingly takes the dimension of kinematic viscosity (length squared per time). From Eq. 11, utilizing the parameters defined in Eq. 12 and 13, we get the following secular equation in terms of the eigenvalues ω^2,

$$\omega^2 = \left(c_0^2 - c_A^2 - \alpha^2 c_3^2\right)k^2 + p^2\left(\omega^2 - c_0^2 k^2\right)\left(\omega^2 - \left(c_1^2 + c_2^2\right)k^2 - \frac{\left(\alpha^2 - \alpha\right)c_3^2}{c_A^2 p^2}\right) - \frac{d^2}{2}k^4 + i\frac{\alpha c_3 d}{2}k^3 \tag{14}$$

Eq. 14 is the dispersion equation for a one dimensional infinite rod formed of dielectric grains, such that it is endowed with dipole and quadrupole densities in an electrostatic condition with constant external electric field. In the absence of external electric field, the dispersion is a function of quadrupole density. Such observation arises from the assumption made in this work that the dipole density is directly related to, while the quadrupole density is independent of the external electric field [2].The corresponding eigenvectors from Eq. 11 comprise the amplitudes of the propagating macro-displacement waves and micro-displacement gradient waves (modes of vibration), respectively. The relationship between the eigenvector components A_1 and B_{11} are given as

$$B_{11} = A_1 \left(\frac{\omega^2 - c_0^2 k^2}{\left(c_A^2 + \alpha^2 c_3^2\right)k - i\frac{\alpha c_3 d}{2}k^2 + \frac{d^2}{2}k^3} \right) \tag{15}$$

for a physically admissible eigenvalue ω^2 which ensures the existence of non-null fields.

Similar to the approach taken in [26], we introduce the dimensionless wavenumber and frequency

$$\xi = pc_0 k \tag{16a}$$

$$\eta = p\omega \tag{16b}$$

We also define dimensionless velocities and a dimensionless term corresponding to the parameter d as follows

$$\begin{aligned} \gamma_A &= \frac{c_A}{c_0} = \sqrt{\frac{Q}{P+Q}}, \quad \gamma_1 = \frac{c_1}{c_0} = \sqrt{\frac{R}{P+Q}}\sqrt{\frac{\rho}{I}} \\ \gamma_2 &= \frac{c_2}{c_0} = \frac{\bar{Q}}{\sqrt{P+Q}}\sqrt{\frac{\rho}{I}}, \quad \gamma_3 = \frac{c_3}{c_0} = \frac{E_1^{(0)}}{\sqrt{P+Q}} \\ \mu &= \frac{d}{pc_0^2} = \frac{\bar{Q}\sqrt{Q}}{P+Q}\sqrt{\frac{\rho}{I}} = \gamma_A\gamma_2 \end{aligned} \tag{17}$$

Using Eq. 16 and 17, Eq. 14 can be recast in the form

$$\eta^2 = \left(1 - \gamma_A^2 - \alpha^2\gamma_3^2\right)\xi^2 + \left(\eta^2 - \xi^2\right)\left(\eta^2 - \left(\gamma_1^2 + \gamma_2^2\right)\xi^2 - \frac{\left(\alpha^2 - \alpha\right)\gamma_3^2}{\gamma_A^2}\right) - \frac{\mu^2}{2}\xi^4 + i\frac{\alpha\gamma_3\mu}{2}\xi^3 \tag{18}$$

Eq. 18 is the dimensionless form of the dispersion relation in Eq. 14. We introduce the parameter

$$B'_{11} = pc_0 B_{11} \tag{19}$$

and the dimensionless parameter

$$\beta = \frac{B'_{11}}{A_1} \tag{20}$$

Now Eq. 15 can be written, using Eq. 16, 17, 19, and 20, as

$$\beta = \frac{\eta^2 - \xi^2}{\left(\gamma_A^2 + \alpha^2\gamma_3^2\right)\xi - i\frac{\alpha\gamma_3\mu}{2}\xi^2 + \frac{\mu^2}{2}\xi^3} \tag{21}$$

Further, the phase and group velocities can be obtained as follows

$$v_p = \frac{\omega}{k}, \quad v_g = \frac{d\omega}{dk} \tag{22}$$

where v_p is the phase velocity, and v_g is the group velocity. Using Eq. 16, the dimensionless form of the phase and group velocities can be written, respectively, as

$$\upsilon_p = \frac{\eta}{\xi}, \quad \upsilon_g = \frac{d\eta}{d\xi} \tag{23}$$

Further, the mechanical energy transfer ratios associated with the micro- and macro-scale degrees of freedom can be obtained, using Eq. 9, 12, 13, and 21 and considering the time average of the mechanical energy density over a time period

$$\frac{E_{micro}}{E_{total}} = \frac{\frac{1}{2T}\int_t^{t+T}\left(I\dot{\psi}\qquad\qquad + R\psi_{11,1}^2\right)dt}{\frac{1}{2T}\int_t^{t+T}\left(I\dot{\psi}\qquad\qquad + R\psi_{11,1}^2 + \rho\dot{\zeta}\qquad\qquad\right)dt} = \frac{\beta^2\left(\gamma_A^2\eta^2 + \gamma_A^2 + \gamma_A^2\gamma_1^2\xi^2\right)}{\beta^2\left(\gamma_A^2\eta^2 + \gamma_A^2 + \gamma_A^2\gamma_1^2\xi^2\right) + \eta^2 + \xi^2 - \gamma_A^2\xi^2} \tag{24a}$$

$$\frac{E_{macro}}{E_{total}} = 1 - \frac{E_{micro}}{E_{total}} = \frac{\eta^2 + \xi^2 - \gamma_A^2\xi^2}{\beta^2\left(\gamma_A^2\eta^2 + \gamma_A^2 + \gamma_A^2\gamma_1^2\xi^2\right) + \eta^2 + \xi^2 - \gamma_A^2\xi^2} \tag{24b}$$

3.2. Results:

From Eq. 17, it is clear that γ_A has lower bound limit of 0 and upper bound limit of 1. Very small values of γ_A represent materials in which the micro-stiffness is negligible compared to their macro-stiffness, and values close to the upper bound level have large micro-stiffness compared to their macro-stiffness. A value of $\gamma_A = 0.71$ corresponds to approximately equal macro- and micro-stiffness of the material. On the other hand γ_1, γ_2, and μ have lower bound of 0 and an upper bound that can theoretically tend to infinity. γ_3 can be any negative or positive value, depending on the sign of the external electric field. For a particular ratio of macro-density to micro-density, larger γ_1 implies a growing dominance of second gradient behavior, while large values of γ_2 and μ imply significant quadrupole effect. Large value for the magnitude of γ_3 imply large external electric field, and large α suggest large polarizability.

To illustrate the effect of the electro-elasticity we study 2 cases with equal micromorphic properties. Case 1 is in a null external electric field, while case 2 is under the effect of a nonzero external electric field. The particular values used for the involved parameters have been chosen to be of the same order of material properties used in [1, 2], except that the electric field and polarizability have been chosen larger in order to facilitate visual comparison. For both cases, the parameters chosen are $\gamma_A = 7.1\times10^{-1}$, $\gamma_1 = 5\times10^{-3}$, $\gamma_2 = 7.6\times10^{-4}$, and $\alpha = 1.0\times10^{-2}$, except that for case 1, $\gamma_3 = 0$ and for case 2, $\gamma_3 = 3.9$. The dispersion curves for both cases 1 and 2 are plotted in Figure 2. Figure 2 implies that the optical branch for case 1 starts at the dimensionless frequency 1, while optical branch for the case 2 starts at a value less than unity. This value can be obtained by introducing $\xi = 0$ in Eq. 18, which gives, for the optical branch,

$$\eta = \sqrt{1+(\alpha)(\alpha-1)\frac{\gamma_3^2}{\gamma_A^2}} \tag{25}$$

Eq. 25 corresponds to the frequency $\omega = \sqrt{\frac{c_A^2+(\alpha)(\alpha-1)c_3^2}{p^2c_A^2}}$. Therefore, the starting dimensionless frequency for the optical branch is only related to the external electric field and the polarizability, with quadrupole density having no effect [27] (considering mechanical

micromorphic properties to be fixed). Clearly, the starting point of the optical wave is dimensionless frequency of 1 when either α or γ_3 vanishes, and can be less or greater than 1 based on whether the value for α is less or greater than unity. However, usual values of α are orders of magnitude smaller than unity. Theoretically, there is a possibility that the expression under the square root in Eq. 25 becomes negative, hence resulting in an imaginary dimensionless frequency with zero real part. The condition for such a possibility is as follows:

$$\left(\alpha-\frac{1}{2}\right)^2+\left(\frac{\gamma_A}{\gamma_3}\right)^2<\frac{1}{4} \tag{26}$$

which simply is the area inside a circle with center of $\left(\frac{1}{2},0\right)$ and the radius of $\frac{1}{2}$ in a coordinate system with a horizontal axis α and a vertical axis $\frac{\gamma_A}{\gamma_3}$ (See Figure 3). In cases where the external electric field is positive (the directions of external electric field and propagating wave are the same) and Eq. 26 is satisfied, the imaginary part of the frequency takes positive values, suggesting instability. If the external electric field is negative, attenuation occurs.

Dimensionless group velocities of the optical branches at small wavenumbers in both cases are zero, therefore, electro-elasticity coupling has no effect on the group velocity of the optical branch at small wavenumbers (See Figure 4a). However, the acoustic branches in cases 1 and 2 have different group velocities at small wavenumbers. Keeping only lower order terms of dimensionless frequency and wavenumber in Eq. 18 results in the dimensionless group velocity of $\sqrt{1-\gamma_A^2\left(\frac{\alpha^2\gamma_3^2+\gamma_A^2}{\alpha^2\gamma_3^2+\gamma_A^2-\alpha\gamma_3^2}\right)}$ (corresponding to the group velocity of $\sqrt{c_0^2-c_A^2\left(\frac{\alpha^2c_3^2+c_A^2}{\alpha^2c_3^2+c_A^2-\alpha c_3^2}\right)}$). This value, keeping the mechanical properties constant (as is for the cases 1 and 2), is a function of only the electric field and polarizability. For vanishing values of the external electric field, case 1 and 2 behave equally at small wavenumbers for the acoustic branch. Quadrupole density, on the other hand, plays no noticeable role in the group velocity of the acoustic branch at small wavenumbers.

The asymptotes of both the optical and the acoustic branches may be found by keeping only higher order terms of the dimensionless frequency and wavenumber in Eq. 18, which, after solving for the dimensionless frequency, gives

$$\eta = \frac{\sqrt{2}}{2}\sqrt{\gamma_1^2+\gamma_2^2+1 \pm \sqrt{\left(\gamma_1^2+\gamma_2^2-1\right)^2+2\mu^2}}\,\xi \tag{26}$$

or $\omega = \frac{\sqrt{2}}{2p}\sqrt{\frac{c_1^2+c_2^2}{c_0^2}+1 \pm \sqrt{\left(\frac{c_1^2+c_2^2}{c_0^2}-1\right)^2+2\frac{d^2}{p^2c_0^4}}}\,k$. Obviously, asymptotes are functions of quadrupole density, but polarizability and the external electric field are not appearing in their expression. The coefficients of ξ in Eq. 26 show the dimensionless group and phase velocities for both cases 1 and 2 at large wavenumbers, as depicted in Figure 4a and b. For the case where γ_2 (and μ) are negligible, Eq. 26 simplifies to

$$\eta = \xi, \quad \eta = \gamma_1\xi \tag{27}$$

(corresponding to asymptotes $\omega = c_0 k$ and $\omega = c_1 k$), which are the asymptotes for a granular material similar to cases 1 and 2, but without dipole and quadrupole densities (only elasticity).

According to Figure 4c and 4d, at small wavenumbers, in both cases 1 and 2, micro-scale degree of freedom is the dominant term playing role for energy transfer in the optical branch, while at large wavenumbers, the macro-scale degree of freedom becomes dominant. For the acoustic branch, micro- and macro-scale degrees of freedom carry almost equal energy at small wavenumbers and the micro-scale's portion increases for larger wavenumbers. External electric field increases micro-scale degree of freedom's energy transfer. This shift, however, is not significant for the two cases studied.

A consequence of electro-elasticity coupling effect can be clearly seen in Figure 2 where the band gap appears to change size and location as a function of external electric field. It is possible, theoretically, to make band gap emerge for a micro-structure that does not exhibit band gap, by using particular value of external electric field (without changing the microstructure and/or dipole and quadrupole densities). The inverse is also true; band gaps can be removed from the dispersion behavior of a granular medium by choosing appropriate value for external electric field. These two

cases have been shown in Figure 5, where only changing external electric field creates (Figure 5a) or removes (Figure 5b) frequency band gaps. Such behavior suggests micro-structures that can be tuned based on the desired response and application. If the directions of external electric field and propagating wave are the same, one must pay heed to the rise of instability introduced by the large electric field value. Considering a stable material with specified polarizability and quadrupole density, effect of the positive external electric field on the emergence of instability is illustrated in Figure 6. The material constants used in the four cases of Figure 6 are similar to the case 2 of Figures 2 and 4, except for the dimensionless parameter γ_3 related to the external electric field. Four different positive values of the parameter γ_3 have been considered and the real and imaginary parts of the dimensionless frequency in the dispersion curve have been plotted, respectively, in Figure 6a and 6b. Clearly, increasing positive external electric field shifts the band gap to smaller frequencies and decreases the dimensionless frequency at which the optical branch starts. Also, as discussed before, a large value of positive external electric field causes the optical wave to become an acoustic wave (depicted in Figure 6 for the cases $\gamma_3 = 6$ and $\gamma_3 = 8$). Such a transition leads to complex frequencies of acoustic wave branch, which have negligible or zero real parts and large values of positive imaginary parts, implying instability caused by the positive external electric field. The instability pertains to the growing of amplitude of the acoustic wave branch with time. Numerical studies suggest a critical point where the instability arises. Figure 7 shows the real and imaginary parts of the dimensionless frequency at dimensionless wavenumber 1 as a function of γ_3 for the optical and acoustic branches (shown in Figure 7a and 7b, respectively). The parameters used are the same as that used in case 2 except for the parameter γ_3 which is taken to be a variable here. According to Figure 7a, the optical branch has a zero imaginary part of the dimensionless frequency and the real part of the dimensionless frequency reduces as the positive external electric field increases. The acoustic wave shown in Figure 7b illustrates a critical point $\gamma_3 = 5.01$ .The real part of the acoustic branch decreases with an increase in the external electric field intensity until it reaches zero at the critical point, and remains zero afterwards. The imaginary part of the dimensionless frequency starts from zero until it reaches the critical point, and obtains positive values for γ_3 beyond the critical point. Clearly, any value taken for γ_3 greater than the critical point results in the emergence of instability. Each set of material parameters results in a different critical point, and must be accounted for when designing or analyzing the granular media or

metamaterials. Since finding possible microstructures for the required desired behavior of the granular medium/metamaterial usually needs optimization algorithms, an inequality constraint to prevent instability can be imposed on the solutions by having the square of the expression of the dimensionless frequency as a function of γ_3 for the acoustic branch be nonnegative. As mentioned before, for the case where the directions of external electric field and propagating wave are opposite (negative external electric field), there is no instability. In this case, the imaginary part of the frequency in the acoustic branch becomes negative, suggesting attenuation.

4. Summary and Conclusions

In the present paper, we have investigated the electro-elasticity coupling effect in the dispersive behavior of a one dimensional infinite medium composed of dielectric grains placed in a constant electric field. The results were compared with a similar granular medium with zero external electric field. Based on the discussion in section 3, polarizability and electric field affect the dispersion curve at small wavenumbers, while quadrupole density is responsible for a change in asymptotes of the two branches at large wavenumbers. Therefore, frequency band gaps may emerge by the electro-elasticity coupling, and by the same token, may be removed from a dispersion curve already exhibiting band gaps. The optical wave may also be altered to behave as an acoustic wave. However, a constraint on the value of the external electric field must be insured to prevent instabilities (refer to Figure 3). The studied problem consider a rod formed of dielectric grains which has no rigid body motion. This assumption yields symmetry in forward and backward waves propagating in the medium. Therefore, we only studied the forward wave propagation. It has been shown that for a moving medium the dispersion becomes asymmetric, leading to different dispersive behavior in the forward and backward propagating waves [28, 29]. Such asymmetry for granular structures will be investigated in future works.

Based on the results and discussion presented in the paper, certain combination of the material constants can lead to a particular class of behavior that is suitable for a purpose of interest. This combination is not unique, and there might be many combinations yielding the same result, thus suggesting a not one-to-one relation between the material constants and the behavior. An advantage of the proposed continuum model is the availability of the explicit form of the functions, thereby promising a complete domain of constants to search for possible solutions (see similar approach exemplified for pantographic material systems in [30]). Such theory-based approaches

are in contrast to certain efforts that proceed by postulating *a priori* certain predetermined sets of microstructures [9, 11] or propose to combine micro-elements [31, 32] to achieve an objective that is circumscribed within a known domain of behaviors without the aid of theories that can predict possibilities beyond those that are already known. The granular micromechanics model extended to account for the electro-elasticity coupling can thus provide an efficient paradigm for analyzing natural granular materials, or designing tunable metamaterials with desired dispersive behavior that may be needed for particular applications.

Acknowledgements
This research is supported in part by the United States National Science Foundation grant CMMI -1727433.

References:

1. Misra, A. and P. Poorsolhjouy, *Granular micromechanics based micromorphic model predicts frequency band gaps.* Continuum Mechanics and Thermodynamics, 2016. **28**(1-2): p. 215-234.
2. Romeo, M., *Microcontinuum approach to electromagneto-elasticity in granular materials.* Mechanics Research Communications, 2018. **91**: p. 33-38.
3. Bazzaz, M., et al., *A Straightforward Procedure to Characterize Nonlinear Viscoelastic Response of Asphalt Concrete at High Temperatures.* Transportation Research Record. **0**(0): p. 0361198118782033.
4. Misra, A., V. Singh, and M.K. Darabi, *Asphalt pavement rutting simulated using granular micromechanics-based rate-dependent damage-plasticity model.* International Journal of Pavement Engineering, 2017: p. 1-14.
5. Kumar Pal, R., et al., *Tunable Wave Propagation in Granular Crystals by Altering Lattice Network Topology.* Journal of Engineering Materials and Technology, 2016. **139**(1): p. 011005-011005-7.
6. Pal, R.K. and P.H. Geubelle, *Wave tailoring by precompression in confined granular systems.* Phys Rev E Stat Nonlin Soft Matter Phys, 2014. **90**(4): p. 042204.
7. Xu, J. and B. Zheng, *Stress Wave Propagation in Two-dimensional Buckyball Lattice.* Scientific Reports, 2016. **6**: p. 37692.
8. Merkel, A., V. Tournat, and V. Gusev, *Experimental Evidence of Rotational Elastic Waves in Granular Phononic Crystals.* Physical Review Letters, 2011. **107**(22).
9. Li, J. and S. Li, *Generating ultra wide low-frequency gap for transverse wave isolation via inertial amplification effects.* Physics Letters A, 2018. **382**(5): p. 241-247.
10. Colombi, A., et al., *Elastic Wave Control Beyond Band-Gaps: Shaping the Flow of Waves in Plates and Half-Spaces with Subwavelength Resonant Rods.* Frontiers in Mechanical Engineering, 2017. **3**(10).
11. An, X., H. Fan, and C. Zhang, *Elastic wave and vibration bandgaps in two-dimensional acoustic metamaterials with resonators and disorders.* Wave Motion, 2018. **80**: p. 69-81.
12. Cummer, S.A., J. Christensen, and A. Alù, *Controlling sound with acoustic metamaterials.* Nature Reviews Materials, 2016. **1**: p. 16001.

13. Chen, Z., et al., *Metamaterials-based enhanced energy harvesting: A review.* Physica B: Condensed Matter, 2014. **438**: p. 1-8.
14. Carrara, M., et al., *Metamaterial-inspired structures and concepts for elastoacoustic wave energy harvesting.* Smart Materials and Structures, 2013. **22**(6): p. 065004.
15. Romeo, M., *A variational formulation for electroelasticity of microcontinua.* Mathematics and Mechanics of Solids, 2015. **20**(10): p. 1234-1250.
16. Romeo, M., *Micromorphic continuum model for electromagnetoelastic solids.* Zeitschrift für angewandte Mathematik und Physik, 2011. **62**(3): p. 513-527.
17. dell'Isola, F., et al., *The complete works of Gabrio Piola: Volume I Commented English Translation - English and Italian Edition*. 2014: Springer Publishing Company, Incorporated. 813.
18. Misra, A. and P. Poorsolhjouy, *Grain- and macro-scale kinematics for granular micromechanics based small deformation micromorphic continuum model.* Mechanics Research Communications, 2017. **81**: p. 1-6.
19. Suiker, A.S.J., R. de Borst, and C.S. Chang, *Micro-mechanical modelling of granular material. Part 1: Derivation of a second-gradient micro-polar constitutive theory.* Acta Mechanica, 2001. **149**(1-4): p. 161-180.
20. Suiker, A.S.J., R. de Borst, and C.S. Chang, *Micro-mechanical modelling of granular material. Part 2: Plane wave propagation in infinite media.* Acta Mechanica, 2001. **149**(1-4): p. 181-200.
21. Misra, A. and P. Poorsolhjouy, *Identification of higher-order elastic constants for grain assemblies based upon granular micromechanics.* Mathematics and Mechanics of Complex Systems, 2015. **3**(3): p. 285-308.
22. Misra, A. and P. Poorsolhjouy, *Elastic Behavior of 2D Grain Packing Modeled as Micromorphic Media Based on Granular Micromechanics.* Journal of Engineering Mechanics, 2016. **143**(1): p. C4016005.
23. Mindlin, R.D., *Micro-Structure in Linear Elasticity.* Archive for Rational Mechanics and Analysis, 1964. **16**(1): p. 51-78.
24. Maugin, G.A., *Continuum mechanics of electromagnetic solids*. Vol. 33. 1988: Elsevier.
25. Chang, C.S. and A. Misra, *Theoretical and Experimental-Study of Regular Packings of Granules.* Journal of Engineering Mechanics-Asce, 1989. **115**(4): p. 704-720.
26. Engelbrecht, J., et al., *Waves in microstructured materials and dispersion.* Philosophical Magazine, 2005. **85**(33-35): p. 4127-4141.
27. Romeo, M., *Acoustic waves in micropolar elastic ferroelectrics.* Mechanics Research Communications, 2015. **63**: p. 33-38.
28. Attarzadeh, M.A. and M. Nouh, *Non-reciprocal elastic wave propagation in 2D phononic membranes with spatiotemporally varying material properties.* Journal of Sound and Vibration, 2018. **422**: p. 264-277.
29. Attarzadeh, M.A. and M. Nouh, *Elastic wave propagation in moving phononic crystals and correlations with stationary spatiotemporally modulated systems.* AIP Advances, 2018. **8**(10): p. 105302.
30. dell'Isola, F., et al., *Pantographic metamaterials: an example of mathematically driven design and of its technological challenges.* Continuum Mechanics and Thermodynamics, 2018: p. 1-34.
31. Matlack, K.H., et al., *Designing perturbative metamaterials from discrete models.* Nature Materials, 2018. **17**(4): p. 323-328.
32. Bilal, O.R., et al., *Intrinsically Polar Elastic Metamaterials.* Adv Mater, 2017. **29**(26).

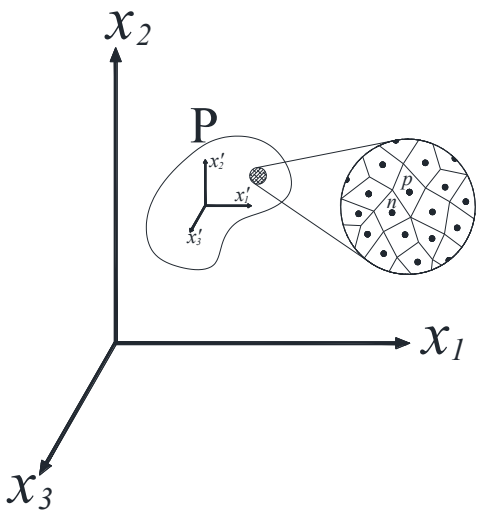

Figure 1- Schematic of continuum material point, P, with its granular microstructure and the coordinate systems *x* and *x'*(from [18])

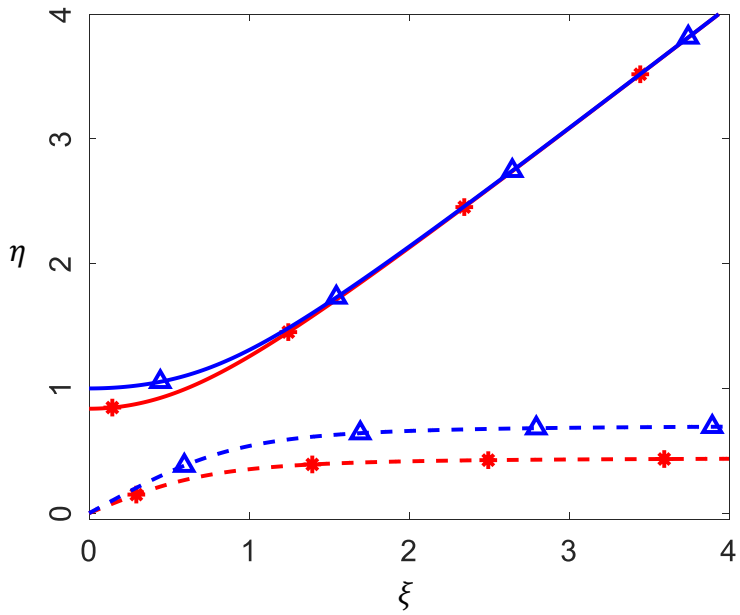

Figure 2- Dispersion curve for cases 1 and 2. Case 1 is depicted by blue lines (marked with triangles), and case 2 by red lines (marked with asterisks). Solid lines and dashed lines represent optical and acoustic branches, respectively.

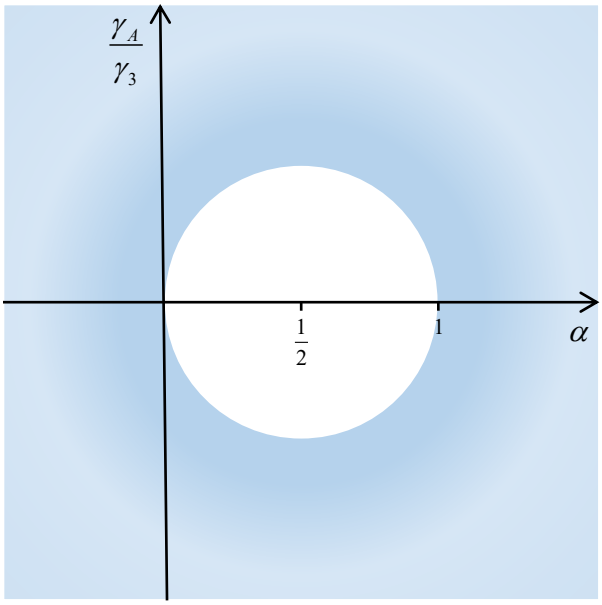

Figure 3- Instability criterion for a positive external electrical field, where any point inside the circle leads to instability.

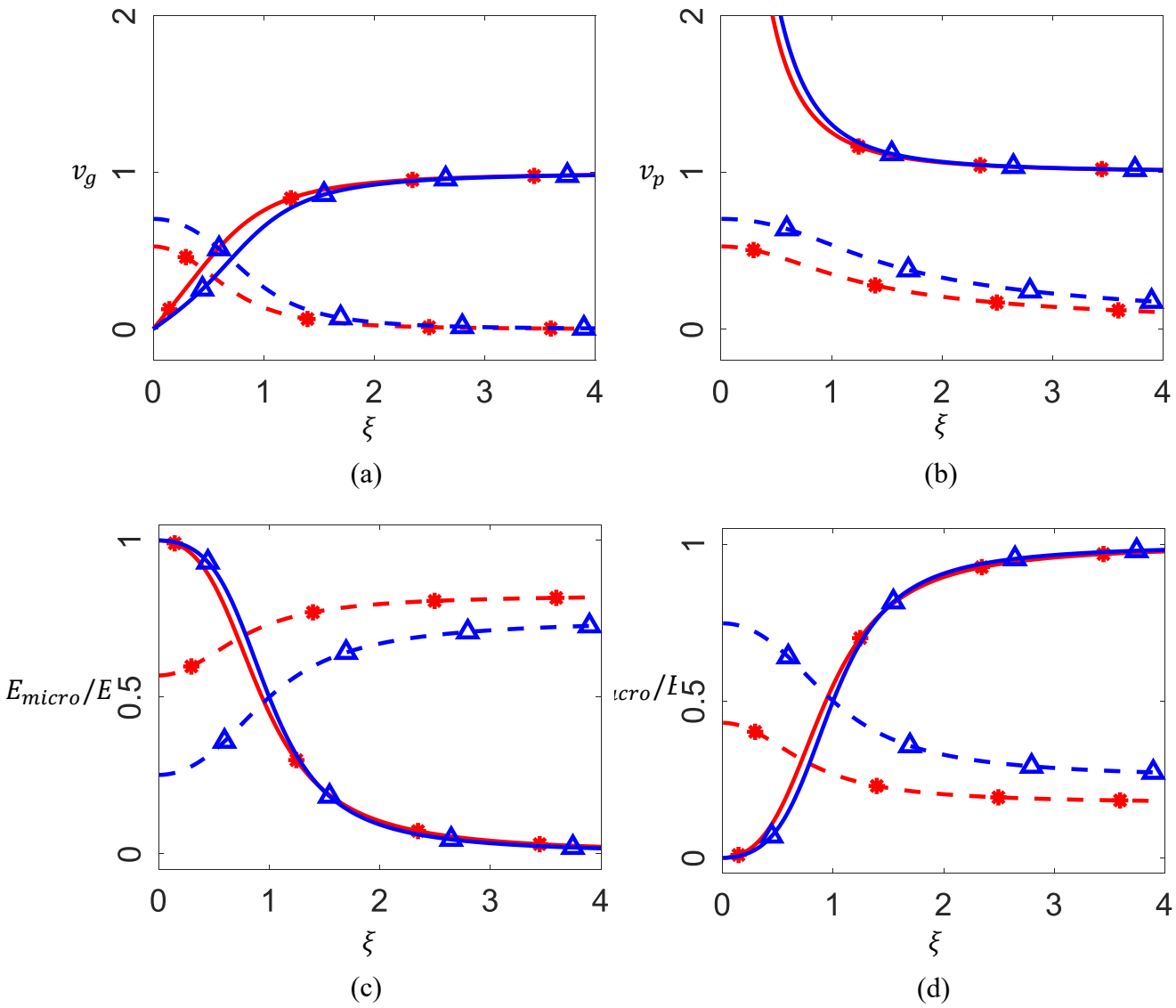

Figure 4- (a) Dimensionless group velocity for cases 1 and 2. (b) Dimensionless phase velocities for cases 1 and 2. (c) Energy transfer ratio associated with the micro-scale degree of freedom to the total energy transferred by the wave, for cases 1 and 2. (d) Energy transfer ratio associated with the macro-scale degree of freedom to the total energy transferred by the wave, for cases 1 and 2. Case 1 is depicted by blue lines (marked with triangles), and case 2 by red lines (marked with asterisks). Solid lines and dashed lines represent optical and acoustic branches, respectively.

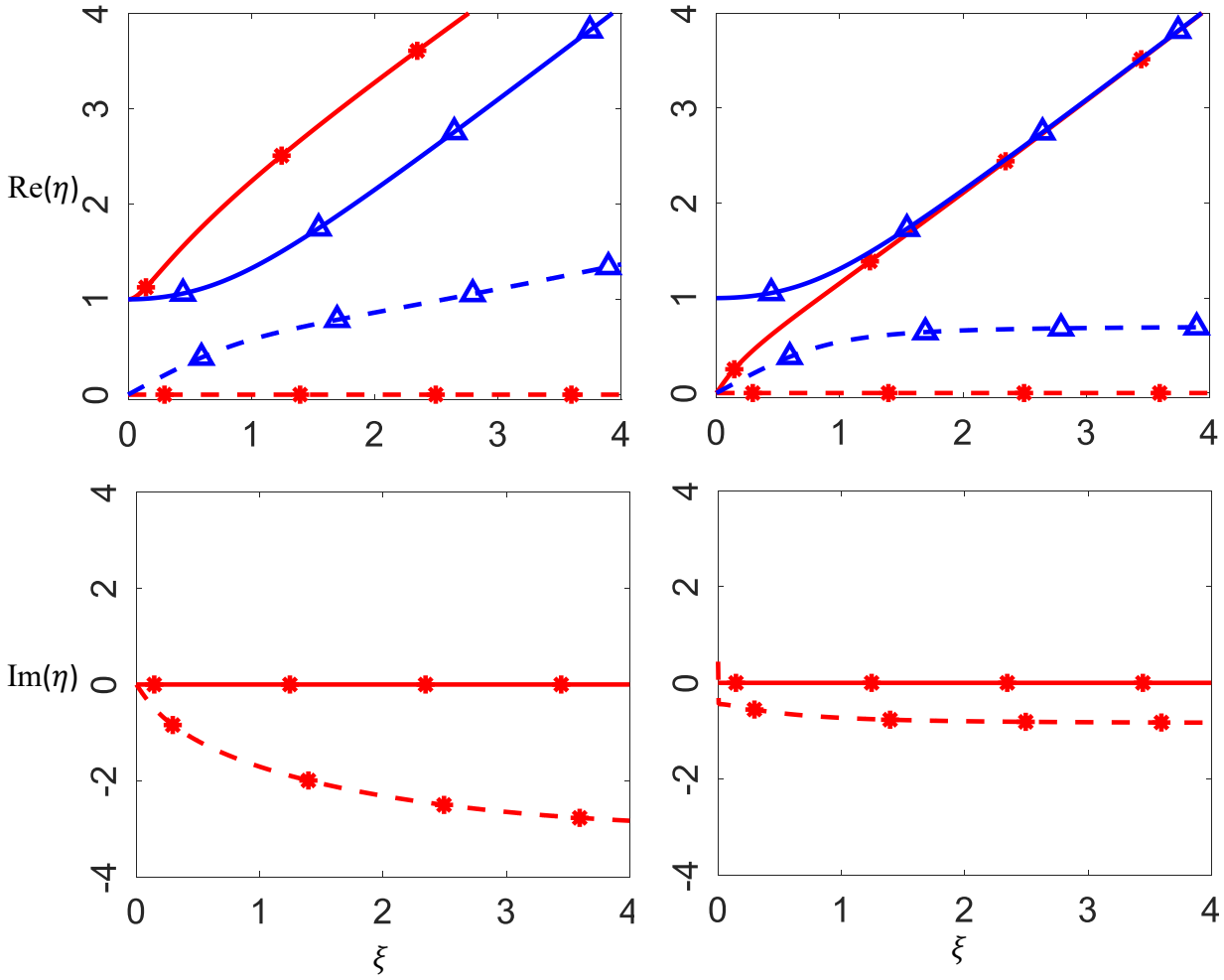

Figure 5- Real and imaginary parts of the dimensionless frequency in the dispersion relation for both optical and acoustic branches where solid and dashed lines represent optical and acoustic branches, respectively. Lines marked with triangle (blue lines) show cases without external electric field and lines marked with asterisk (red line) show the effect of external electric field in electro-elasticity coupling (a) emergence of frequency band gap. Material parameters chosen are $\gamma_A = 0.71, \gamma_1 = 0.3, \gamma_2 = 0.00076, \gamma_3 = -3.9, \alpha = 1.01$, where for the case with zero external electric field the parameter γ_3 is zero (b) removing frequency band gap. Material Parameters chosen are $\gamma_A = 0.71, \gamma_1 = 0.005, \gamma_2 = 0.00076, \gamma_3 = -7.8, \alpha = 0.01$, where for the case with zero external electric field the parameter γ_3 is zero.

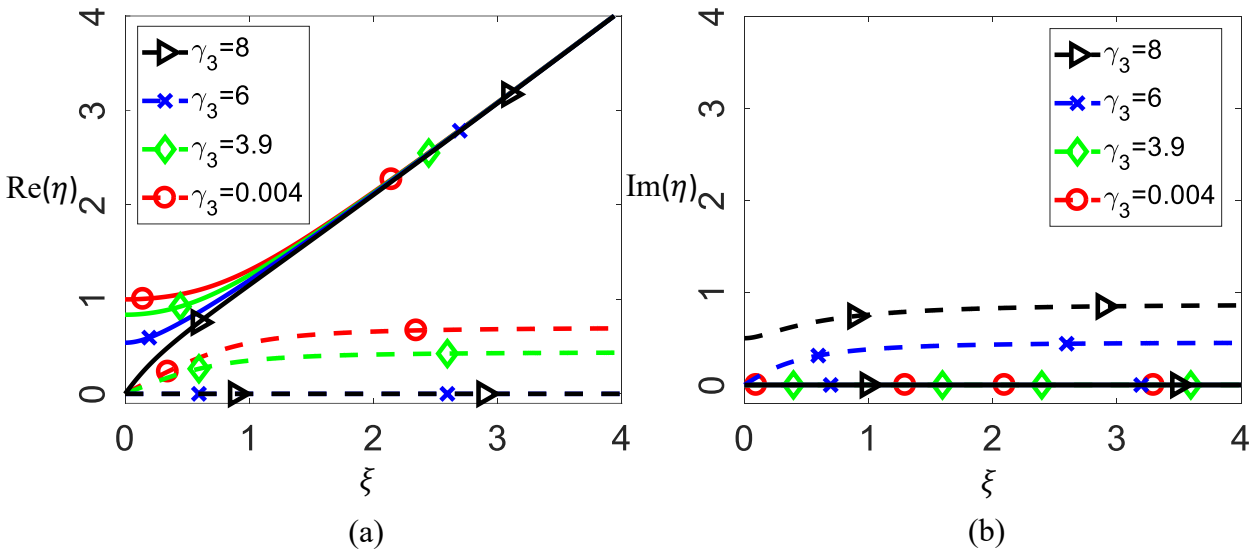

Figure 6- Dispersion curve for four different cases of external electric field (that is proportional to γ_3) where (a) shows the real part of the frequency and (b) shows the imaginary part of the frequency in the dispersion curve. Solid and dashed lines represent optical and acoustic branches, respectively. The parameters used are equal to case 2 except for γ_3 which is taken to be variable.

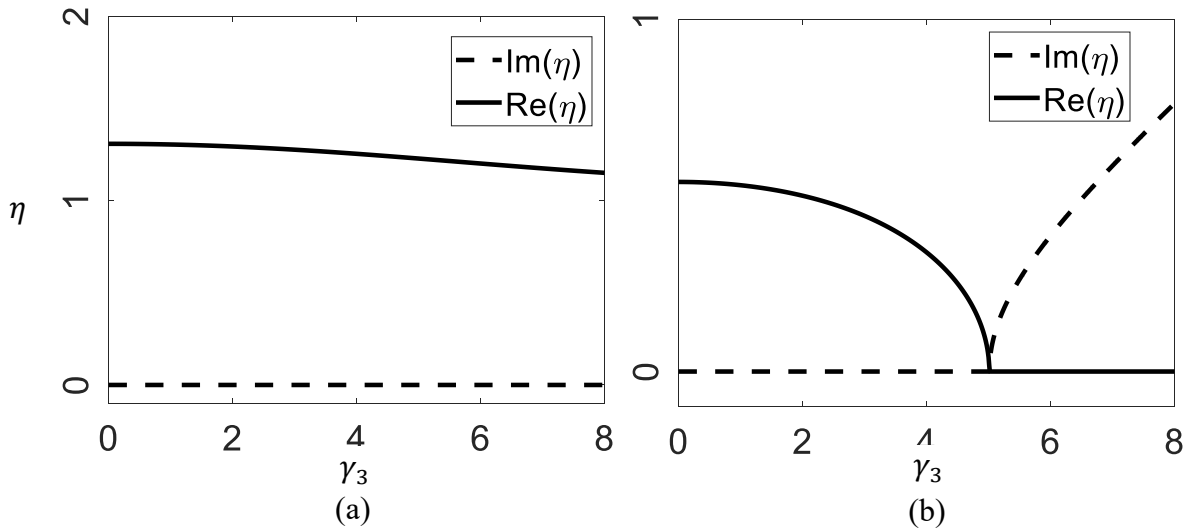

Figure 7- Real and imaginary parts of the dimensionless frequency at dimensionless wavenumber 1 as a function of γ_3 for (a) the optical branch and (b) the acoustic branch. The parameters used are equal to case 2 except for γ_3 which is taken to be variable.